JOURNAL OF THERMOPHYSICS AND HEAT TRANSFER
Vol. 21, No. 4, October–December 2007

Effectiveness Distributions on Turbine-Blade Cascade Platforms Through Simulated Stator–Rotor Seals

Lesley M. Wright*
University of Arizona, Tucson, Arizona 85721-0119
and
Sarah Blake† and Je-Chin Han‡
Texas A&M University, College Station, Texas 77843-3123

DOI: 10.2514/1.30382

A five-blade linear cascade is used to experimentally investigate turbine-blade platform cooling. Three slot configurations placed upstream of the blades are used to model advanced seals between the stator and rotor. The seal configurations include vertical injection of the coolant onto the platform, a redirection of the coolant onto the platform, and a labyrinthlike configuration between the stator endwall and rotor platform. The coolant flow rate through the seals varies from 0.5 to 2.0% of the mainstream flow. The film-cooling effectiveness is measured on the platform using pressure-sensitive paint. The upstream slots cover 1.5 passages with the coolant exiting the slot 3.87 cm upstream of the leading edge of the blades. The mainstream Reynolds number is 3.1×10^5 based on the inlet velocity and the chord length of the scaled high-pressure turbine blade. With the pressure-sensitive-paint measurement technique, the effect of the passage-induced secondary flow on the film-cooling effectiveness is easily captured, as the distribution of the film effectiveness is very nonuniform through the passage. In addition, the more advanced seal configurations, considered in the present study, yield reduced film-cooling effectiveness compared with the more fundamental inclined slot configurations.

Nomenclature

C = true chord length of the blade
C_{ax} = axial chord length of the blade
C_{mix} = oxygen concentration of the mainstream-coolant mixture
C_∞ = oxygen concentration of the mainstream
I_{air} = light intensity measured with air injection
I_{N_2} = light intensity measured with nitrogen injection
I_{ref} = light intensity measured at the reference condition (no mainstream, no coolant flows)
l_s = slot length
M_s = slot injection blowing ratio, $\rho_s V_s/\rho_m V_{m1} \cong V_s/V_{m1}$
m_s = slot injection mass flow ratio (percentage of the mainstream flow)
P_{O_2} = partial pressure of oxygen
$P_{O_2 ref}$ = partial pressure of oxygen at the reference condition (no mainstream, no coolant flows)
Re = mainstream flow Reynolds number based on the inlet velocity and axial chord length
s = slot width, m
V_{m1} = mainstream velocity at the cascade inlet, m/s
V_{m2} = mainstream velocity at the cascade exit, m/s
V_s = slot injection velocity, m/s
w = slot width, m
x = axial distance from the cascade leading edge, m
η = film-cooling effectiveness
ρ_m = density of the mainstream, kg/m^3
ρ_s = density of the slot coolant, kg/m^3

Presented as Paper 3402 at the 9th AIAA/ASME Joint Thermophysics and Heat Transfer Conference, San Francisco, CA, 5–8 June 2006; received 10 February 2007; revision received 2 May 2007; accepted for publication 2 May 2007.

*Assistant Professor, Department of Aerospace and Mechanical Engineering. Member AIAA.
†Graduate Research Assistant, Turbine Heat Transfer Laboratory, Department of Mechanical Engineering.
‡M.C. Easterling Endowed Chair and Distinguished Professor, Turbine Heat Transfer Laboratory, Department of Mechanical Engineering. Associate Fellow AIAA.

I. Introduction

AS ECONOMIES across the world continue to grow, the demand for power also continues to increase. Commercial, industrial, and residential customers have come to expect uninterrupted electrical service required to meet a variety of needs; however, the demand for power is growing faster than the power supply. Meanwhile, the commercial airline industry is facing numerous hurdles and the military is facing new challenges. The common bond between land-based power generation and aircraft propulsion is gas turbine engines. With gas turbines also being used for marine propulsion and scores of other specific industrial applications, it is vital that these engines operate efficiently. The efficiency of a gas turbine engine can be increased by raising the temperature of the hot gases at the inlet of the turbine. However, increasing the temperature of the mainstream gas must be done cautiously, because additional problems can develop. The metallic turbine components must be protected to survive prolonged exposure to the hot gases. The life of the turbine airfoils can be increased by implementing any of a variety of cooling techniques. As presented by Han et al. [1], air is extracted from the compressor and used to cool the airfoils. This coolant air is injected into the hollow airfoils and circulates through internal cooling passages of the blades and vanes. The coolant is discharged through discrete holes in which it forms a protective film on the outer surface of the airfoil. Many investigations have focused on increasing the heat transfer enhancement within the blades via rib turbulators, jet impingement, and pin fins. Also, film cooling has been studied for many years to determine the optimal hole configuration and flow conditions to maximize the protection of the coolant.

With the increasing temperature of the mainstream gases exiting the combustor, the stator vanes and rotor blades must be protected so that they can survive the extreme temperatures. Recently, the blade platform has received renewed attention for an adequate cooling scheme. The vane endwall and the blade platforms comprise a large percentage of the area exposed to the hot mainstream gases. There is a

strong potential for "hot spots" to form on the endwalls and platforms. Over this large area, it is vital to have accurate heat transfer distributions so that efficient cooling schemes can be developed. The cooling schemes should adequately protect the platforms while minimizing the amount of coolant.

A general review of platform (endwall) flow, heat transfer, and film cooling has been completed by Han et al. [1] and Chyu [2]. Several of the papers reviewed by these sources will be considered along with other papers to develop a foundation for platform flow and heat transfer. The secondary flow in a turbine passage is very complex and varies based on the blade profile being considered. Langston et al. [3,4] performed flow measurements to gain insight into this complex secondary flow. They showed that at the inlet of the passage, the boundary splits at the leading edge of the blade. A horseshoe vortex forms, with one leg on the pressure side of the blade and the other leg on the suction side of the blade (in the adjacent passage). The pressure-side leg of the horseshoe vortex travels from the pressure side of the passage to the suction side; this pressure-side leg of the horseshoe vortex becomes known as the passage vortex. This passage vortex will eventually meet the suction-side leg of the horseshoe vortex that has remained near the junction of the suction surface and endwall. Goldstein and Spores [5] also studied the flow through a blade passage. They identified multiple "corner" vortices that developed throughout the passage. A pressure-side corner vortex develops just downstream of the leading edge, and the vortex carries about one-third of the chord length. Two suction-side corner vortices develop along the suction surface in the latter half of the passage. After the passage vortex carries to the suction side of the passage, it lifts from the endwall surface. Below the passage vortex, along the junction at which the suction surface meets the endwall, suction-side counter-rotating corner vortices form.

The highly complex, three-dimensional flow has a strong influence on the heat transferred from the mainstream flow to the blade platform. Blair [6] pioneered the study of endwall heat transfer. He found significant variation of the heat transfer coefficient across the passage and downstream to the trailing edge of the vane, due to the secondary flow along the endwall. Graziani et al. [7] also reported large variations in the endwall heat transfer coefficients. They showed that the heat transfer coefficients on the suction surface of the blade are also influenced by the secondary flow through the passage; however, the heat transfer coefficients on the pressure surface are not affected by the strong secondary flows. Using a mass transfer technique, Goldstein and Spores [5] showed that as the boundary layer splits to form the two legs of the horseshoe vortex near the leading edge of the blades, the heat transfer coefficients increase, and the greatest heat transfer enhancement on the endwall occurs near the leading edge. Other variations are present on the endwall, due to the path of the passage and corner vortices. In addition, near the trailing edge of the blade, the heat transfer coefficients are elevated as the two flows from the two passages meet at the trailing edge. The heat transfer coefficients were also measured on the endwall of a vane passage [8–10]. Similar variations were found, because the heat transfer continues to be dominated by the secondary flow. When the effect of freestream turbulence was considered [9,10], it was found that increasing the turbulence intensity increases the heat transfer coefficients on the passage endwall. However, the effect of the freestream turbulence intensity was minimal near the leading edge and near the suction surface, on which the horseshoe and passage vortices dominate the heat transfer behavior.

With the local areas of high heat transfer identified, film cooling can be implemented on the blade platform to reduce the heat load in these areas. Takieshi et al. [11] obtained heat transfer and film-effectiveness distributions on a vane endwall with discrete film-cooling holes placed at three locations in the passage. They found that the effectiveness is very low near the leading edge on the suction side; with the rollup of the horseshoe vortex, the film coolant lifted from the surface and offered little or no protection. The path of the coolant was also influenced by the passage vortex transporting the coolant from the pressure to the suction side of the passage. Harasgama and Burton [12] used film cooling near the leading edge, just inside the passage, with the film-cooling holes located along an iso-Mach line. Although the row of film-cooling holes was evenly distributed to span the passage, no coolant reached the pressure side of the passage. The film-cooling configuration used by Jabbari et al. [13] consisted of discrete holes placed on the downstream half of the passage. Similar to the upstream design [12], the film-cooling effectiveness varied significantly through the passage, with the coolant moving to the suction side of the passage.

Friedrichs et al. [14–16] studied the film-cooling effectiveness using the ammonia and diazo technique. They found that a simple layout of the film-cooling holes throughout the passage can result in areas being overcooled (or undercooled), due to the secondary flow. With their proposed "improved design," the film holes were placed so that the strong secondary flow could be used advantageously. Using the same amount of coolant, they were able to provide improved coolant coverage. Recently, Barizozzi et al. [17] compared the film-cooling effectiveness on a passage endwall with cylindrical or fan-shaped film-cooling holes. With their cooling designs, they showed that by increasing the blowing ratios, the passage vortex is weakened and the passage cross flow is reduced; therefore, coolant coverage is more uniform across the passage. Similar to flat-plate film cooling, shaped film-cooling holes offer better protection than cylindrical holes.

A similarity between the vane endwall and the blade platform is the existence of a slot (or gap) upstream of the airfoil leading edge. A gap is commonly in place in the transition from the combustion chamber to the turbine vane (stator). Similarly, a gap exists between the stator and rotor, and so the turbine disk can rotate freely. To prevent ingestion of the hot mainstream gases, it is a common practice to inject coolant air through these slots. If this preventive measure is used properly, unnecessary discrete film holes can be eliminated so that coolant is not wasted by overcooling areas on the rotating platform. Blair [6] also measured the film-cooling effectiveness with upstream injection in his pioneering study; he showed large variations in the film-cooling effectiveness over the entire passage, due to the strong secondary flow. Roy et al. [18] placed coolant slots upstream of their vane. They showed the heat transfer near the leading edge was reduced, due to the secondary air injection. Because the slots were placed directly upstream of the blades, a large area in the center of the passage did not receive adequate film-cooling coverage. Slot injection has been the focus of many studies performed at the University of Minnesota [19–21]. They found that using slots, which span the majority of the passage upstream of their vanes, can provide film coverage over most of the passage to the trailing edge of the vane [19,20]. They also found that increasing the amount of coolant through the slot can reduce the effect of the secondary flow. In addition, strategically blocking the slot so that the coolant does not exit the slot uniformly provides thermal advantages (and disadvantages) [21].

The heat transfer coefficients and the film-cooling effectiveness were measured on an endwall of a vane passage with film cooling combined with upstream slot injection by Nicklas [22]. He found that in the upstream region, the film-cooling effectiveness was elevated, due to the large amount of cooling flow from the slot. However, the effectiveness near the discrete holes located near the center of the passages suffered, due to the passage vortex. Liu et al. [23] used a high volume of discrete holes upstream of their vanes to emulate the effect of upstream slot injection. They determined that the film-cooling effectiveness was primarily affected by the blowing ratio of the injection; in addition, as the blowing ratio increases, the uniformity of the coverage increases.

The film-cooling effectiveness has been measured using pressure-sensitive paint (PSP) by Zhang and Jaiswal [24] and Zhang and Moon [25]. They first measured the effectiveness with two upstream injection geometries: two rows of discrete holes and a single-row slot. The effect of a backward-facing step was also considered with the discrete hole configuration. They confirmed that increasing the coolant flow can significantly increase the effectiveness, and they reported that the use of a backward step significantly decreases the effectiveness within the passage. Knost and Thole [26] showed that with increased slot flow, the critical areas of the leading-edge and pressure-side junction can be adequately cooled.

Wright et al. [27] recently applied the PSP technique to measure the film-cooling effectiveness on the blade platform with combined upstream injection (through an inclined slot) and downstream discrete film-cooling holes. They concluded that using the available purge flow coupled with limited discrete film cooling downstream can significantly reduce the amount of coolant required to protect the platform. The PSP technique proved satisfactory in capturing the effect of the passage-induced secondary flow on the film-cooling effectiveness.

As designers strive to push the limits to more efficient engines, more studies of the vane endwall and blade platform have emerged. Although significant effort has been directed to obtaining heat transfer coefficient and film-effectiveness distributions on the endwalls and platforms, the majority of investigations have only considered idealistic geometries. Although incline and vertical slots may be simple to replicate in a laboratory environment, they do not model the advanced seals designed to prevent ingestion of the hot mainstream gases into the engine cavity. Therefore, it is vital to provide designers with detailed film-cooling-effectiveness distributions that are obtained from more advanced seal configurations.

From previous studies, pressure-sensitive paint has proven to be a valuable tool to obtain detailed film-cooling-effectiveness distributions. This technique will again be used to measure the film-cooling effectiveness on turbine-blade platforms with three different stator–rotor seal configurations. A seal that injects the coolant vertically through the platform, a seal that redirects the coolant onto the platform, and a labyrinthlike seal will be used to obtain detailed film-cooling-effectiveness distributions on a blade platform within a linear cascade.

II. Experimental Facility

A. Low-Speed Wind Tunnel

An existing low-speed wind-tunnel facility was used to study the platform film-cooling effectiveness, and a schematic of the facility is shown in Fig. 1. Modifications were made to the endwall of the wind tunnel that was previously used by Wright et al. [27]. The open-loop wind tunnel operates in suction with two mesh screens located at the inlet of the wind tunnel. To produce uniform flow entering the cascade, a 4.5:1 contraction nozzle guides the flow to the linear cascade. The test area is 25.4 cm high by 75.0 cm wide and has a 107.49-deg turning angle to match the turning of the five-blade cascade. Head- and tailboards guide the flow into the cascade. The cascade inlet velocity was maintained at 20 m/s and was set using a variable frequency controller attached to the 15-hp (11.2-kW) blower. The inlet velocity was measured (and continuously monitored) using a pitot tube placed inside the wind tunnel. The mainstream accelerates through the cascade, and so the mainstream velocity at the cascade exit is 50 m/s.

B. Linear Cascade Design

Figure 2 shows the typical advanced high-pressure turbine blade used for this study. The blade, which was scaled up five times, has a 107.49-deg turning angle with an inlet flow angle of 35 deg and an outlet flow angle of −72.49 deg. The chord length of the blade is 22.68 cm and the height of the blade is 25.4 cm. The blade-to-blade spacing at the inlet is 17.01 cm with a throat-to-span ratio of 0.2. The mainstream flow accelerates from 20 m/s at the inlet to 50 m/s at the outlet of the cascade. The inlet flow periodicity and uniformity for the blade design have been measured and reported by Zhang and Han [28]. In addition, the velocity (pressure) distributions along the pressure and suction surfaces of the blades have also been measured. The mainstream Reynolds number (based on the inlet velocity and blade chord) is 3.1×10^5, and the turbulence intensity at the inlet of the cascade is 0.75% [28].

C. Stator–Rotor Seal Configurations

To study the film-cooling effectiveness on the blade platform, the platform was altered so that the advanced seal configurations could be considered upstream of the blades. Three separate seals are considered in the present study. The complexity of the seals gradually increases to the most complex design, which most closely models actual engine seals. For all cases, the upstream seal shown in Fig. 2 covers 1.5 passages, and the seals are located 3.87 cm upstream of the blades (Fig. 3).

The first seal injects the coolant vertically into the mainstream flow, as shown in Fig. 3a. The slot width is 0.44 cm, and the coolant travels 1.91 cm through the slot, and so $l_s/w = 4.34$. The second seal actually redirects the coolant just before it is injected onto the

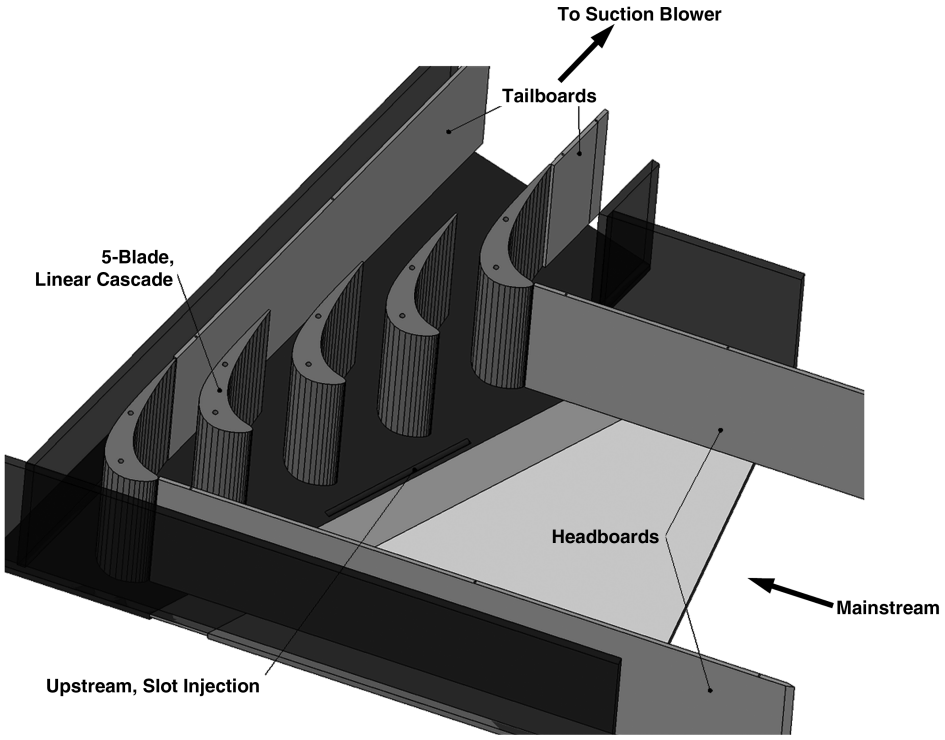

Fig. 1 Overview of the low-speed wind tunnel used to study platform cooling.

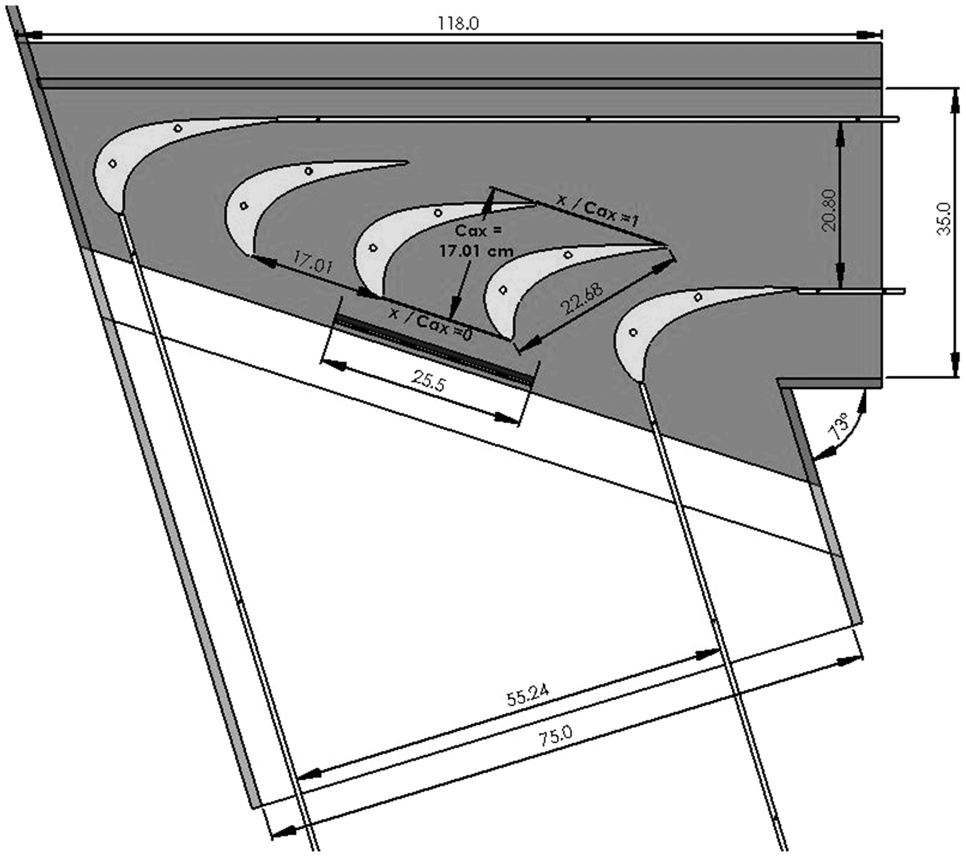

Fig. 2 Low-speed wind-tunnel and turbine-blade details.

platform. As shown in Fig. 3b, the coolant is not directly injected into the mainstream flow. This redirection gives a slot length-to-width ratio of 4.84. The third configuration is the most advanced seal configuration. Figure 3c shows a configuration that models a labyrinth seal, which is the most likely configuration encountered in actual engines. The coolant is actually turned 180 deg before it is expelled onto the platform. In this case, the distance the coolant travels through the seal increases, and so the length-to-width ratio increases to 6.84. Although the length of the flow path increases, due to the redirection of the labyrinth seal, the length of the seal is not sufficient to allow the fluid to hydrodynamically develop.

Coolant (air or nitrogen) is metered through a square-edged orifice flow meter by the American Society of Mechanical Engineers and piped to a plenum located directly beneath the slot. The plenum is sufficiently large enough to ensure that the coolant is uniformly distributed at the exit of the slot. The flow rate of the slot coolant can be varied so that the film-cooling effectiveness can be measured over a range of flow rates varying from 0.5 to 2.0% of the mainstream flow.

III. Pressure-Sensitive-Paint Measurement Technique

The film-cooling effectiveness has been measured using an array of measurement techniques over several decades. Thermocouples, thermochromatic liquid crystals, infrared thermography, and temperature-sensitive paint have been used for surface-temperature measurements that can be converted to the film-cooling effectiveness with knowledge of the mainstream and coolant flows. Although these techniques can be used to obtain the film-cooling effectiveness, the accuracy near the film-cooling holes is questioned. Near the holes, the test material can very thin, and therefore heat conduction through the test surface can give false representations of the film-cooling effectiveness. This is a problem that is an inherent to heat transfer experiments.

Numerical correction of the film-cooling data is one alternative for producing more accurate film-cooling data. Another alternative is to avoid heat transfer experiments. This approach was used by Zhang et al. [24,25] as they used PSP to measure the film-cooling effectiveness on a cascade endwall. Wright et al. [29] used PSP to film the cooling effectiveness on a flat plate with compound-angle film-cooling holes, and they provide a detailed review of the PSP theory and application. In addition, PSP has also been used to measure the effectiveness on a cylinder placed in a low-speed wind tunnel [30]. Both of these studies demonstrate the superiority of PSP measurements compared with other traditional measurement techniques, including steady-state liquid crystal thermography, steady-state infrared thermography, and transient infrared thermography. The PSP technique has also been applied by Ahn et al. [31,32] to measure the film-cooling effectiveness on the leading edge of a rotating blade placed in a three-stage research turbine. Additional film-cooling-effectiveness distributions have been obtained in a blowdown facility on the blade tip [33,34].

The premise behind PSP is an oxygen-quenching effect. As the oxygen partial pressure of the gas in direct contact with the surface increases, the intensity of light emitted by the PSP decreases (hence, oxygen quenched). The PSP can be calibrated to determine the relationship between the emission intensity of the paint and the surrounding oxygen pressure. A test plate is sprayed with the Uni-FIB PSP (UF470-750) supplied by Innovative Scientific Solutions, Inc. and placed inside a vacuum chamber. At each measurement point, the PSP sample was excited using a strobe light equipped with a 500-nm broadband pass filter. A charge-coupled device (CCD) camera with a 630-nm filter records the intensity emitted by the PSP. Figure 4 shows a typical calibration curve relating a known pressure ratio to a measured intensity ratio (for which the reference conditions are taken at atmospheric pressure). At the reference condition, the intensity of light typically measures approximately 90, whereas the maximum intensity measured in the calibration and actual test is 650 and 530, respectively.

After the PSP has been properly calibrated, the film-cooling effectiveness can be measured on the desired test surface. Because of the size of the endwall passage, two sets of images are required to

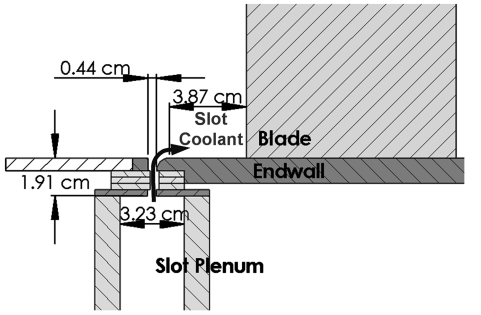

a) Vertical injection

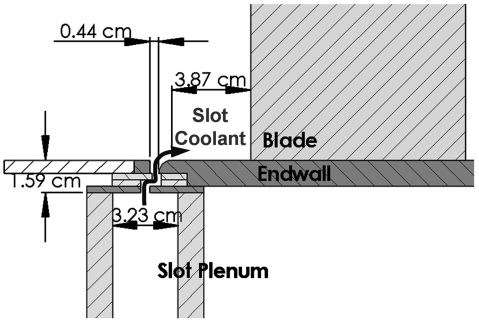

b) Redirected injection

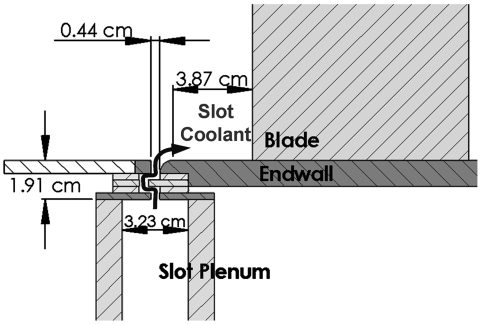

c) Labyrinth injection

Fig. 3 Stator–rotor seal configurations.

capture the entire passage. The procedure to measure the effectiveness on both the upstream and downstream halves of the passage are identical, and the results are combined to give a complete picture of the film-cooling effectiveness on the platform. The film-cooling effectiveness is measured based on a mass transfer technique. Two similar tests are required to calculate the film-cooling effectiveness: one with air as the coolant and one with nitrogen as the coolant. The film-cooling effectiveness can be calculated based on the concentration of oxygen, which is related to the partial pressure of oxygen. Therefore, the film-cooling effectiveness can be calculated using Eq. (1):

$$\eta = \frac{C_\infty - C_{\text{mix}}}{C_\infty} = \frac{(P_{O_2})_{\text{air}} - (P_{O_2})_{N_2}}{(P_{O_2})_{\text{air}}} \approx 1 - \frac{I_{\text{air}}}{I_{N_2}} \tag{1}$$

To accurately determine the film-cooling effectiveness, a total of four images are required: 1) a black image to remove any background noise from the optical components (no mainstream flow, no coolant flow, no excitation light), 2) a reference image to establish the intensity at the reference atmospheric pressure (no mainstream flow, no coolant flow, PSP is excited with the strobe light), 3) an air image to measure the partial pressure of oxygen with air as the coolant (mainstream flow, air as coolant flow, excitation by strobe light), and 4) a nitrogen image to measure the partial pressure of oxygen with nitrogen as the coolant (mainstream flow, nitrogen as coolant flow, excitation by strobe light). As shown in Fig. 4, in the presence of oxygen, the emission intensity falls and the intensity ratio I_{ref}/I increases, as shown by representative point for film cooling with air

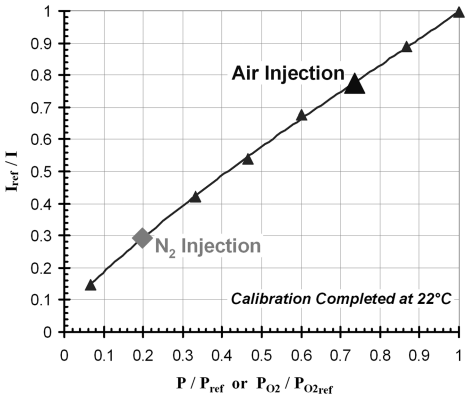

Fig. 4 Pressure-sensitive paint calibration curve.

injection. When nitrogen is injected as the coolant, the emission intensity increases (due to the lack of oxygen), and the intensity ratio decreases, as shown by the point for nitrogen injection. The partial pressure of oxygen with air or nitrogen injection is determined based on the calibration of the emission intensity and pressure. The film-cooling effectiveness can be determined at every pixel, giving a detailed film-cooling-effectiveness distribution on the passage endwall.

Experimental uncertainty was considered using a 95% confidence level, as presented by Coleman and Steele [35]. The uncertainty of the film-effectiveness measurements varies depending on the intensity level measured by the CCD camera. The experimental uncertainty is less than 2% for film-effectiveness measurements greater than 0.5. However, as the effectiveness begins to approach zero (where the measured light intensities are relatively low), the uncertainty rises. For a film-cooling effectiveness of 0.07, the uncertainty is approximately 10% and continues to rise as the effectiveness approaches zero. Although the results presented in the upcoming figures represent single experiments, all of the experiments were repeated to confirm the repeatability of the data. The data proved to be repeatable for the entire range of film effectiveness that was measured.

IV. Results and Discussion

As previously described, the film-cooling effectiveness is measured on a blade platform with three different stator–rotor seal configurations. The detailed film effectiveness is presented for each configuration over the range of coolant flow rates. Following the discussion of the detailed effectiveness distributions, the seal configurations will be compared, based on the laterally averaged film-cooling effectiveness through the passage. The film effectiveness obtained from the present three configurations will also be compared with the film effectiveness resulting from more simplistic (or fundamental) seal configurations.

A. Vertical Injection

The film-cooling effectiveness measured on the platform with vertical coolant injection upstream of the blades is shown in Fig. 5. As Fig. 5a shows, at the lowest coolant flow rate of 0.5%, coolant exits over the entire length of the slot; however, the coolant does not exit the slot uniformly. In addition, the film-cooling effectiveness quickly decays from the seal through the passage. From the PSP measurement, the strong effect of the passage-induced secondary flow on the film-cooling effectiveness is seen. The coolant is carried from the pressure side of the passage to the suction side with the passage vortex. At this low flow rate, a large area of the passage, both along the pressure side and trailing edge, is left unprotected and exposed to the mainstream gas. Similar trends have been observed with other cooling configurations.

Increasing the coolant flow rate increases the coverage area in the passage. As Fig. 5b shows, more area near the pressure side of the passage is covered by the coolant. However, the same behavior of the

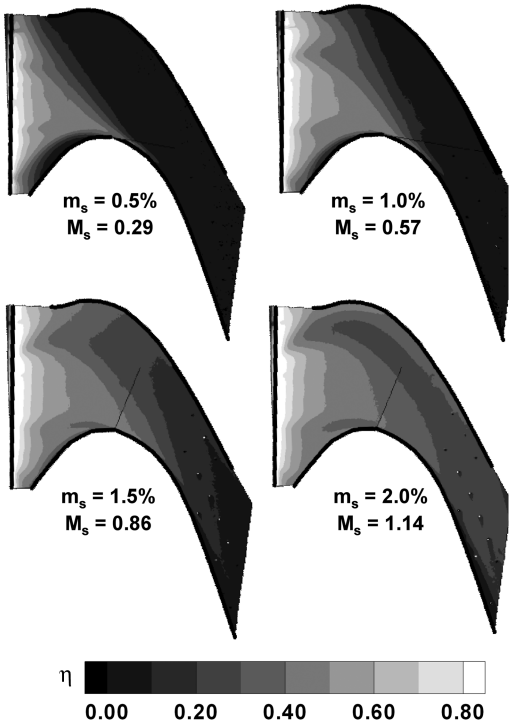

Fig. 5 Measured film-cooling effectiveness with vertical upstream injection.

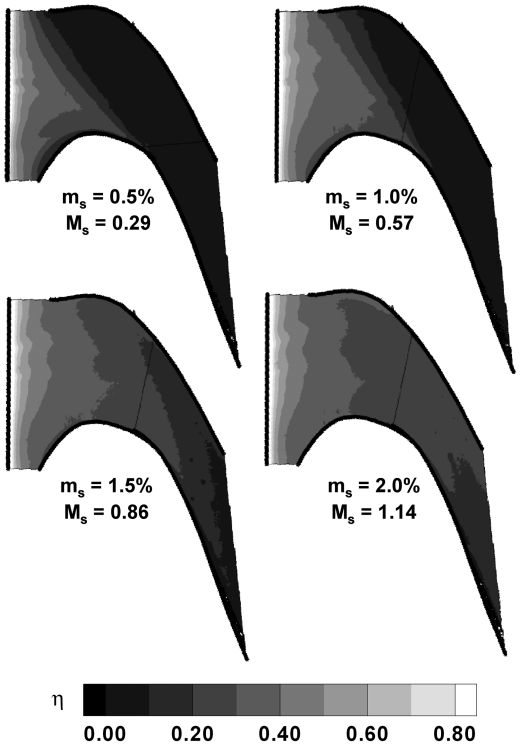

Fig. 6 Measured film-cooling effectiveness with redirected upstream injection.

coolant being forced to the suction side is still observed. Further increasing the flow rate to 1.5% of the mainstream flow (Fig. 5c) yields increased film-cooling effectiveness on the upstream half of the passage with the film penetrating further downstream. Increasing the coolant flow rate also reveals how nonuniformly the coolant exits the slot. As shown in Fig. 5d, a large area of relatively low effectiveness develops near the pressure side of the passage. With the coolant being injected into the mainstream upstream of the blades, the path of the coolant is heavily influenced by the formation of the horseshoe vortex. As Friedrichs et al. [14] showed from oil and dye surface visualizations, the horseshoe vortex forms in the stagnation region upstream of the blade. With this vertical injection of the coolant, there is strong interaction between the coolant and the mainstream. With the formation of the horseshoe vortex, the pressure-side leg becomes the passage vortex as it moves from the pressure to the suction side of the passage. This passage-induced flow carries the majority of the coolant from the pressure side of the passage to the suction side. Downstream of the passage vortex, near the pressure side of the passage, a large area of relatively low film-cooling effectiveness is present. With the large amount of coolant from the seal, 100% of the coolant is not swept to the suction side of the passage. Although the effectiveness is less near the pressure side, the film-cooling effectiveness is not zero.

At the largest flow rate of 2.0% of the mainstream flow, the passage is completely covered from the leading edge to the trailing edge. However, if the present results are compared with an inclined slot [27], the effectiveness near the trailing edge is much lower for this vertical injection at a given flow rate. This should be expected, because with the present vertical injection, the coolant tends to blow off the platform, and the cooling advantage is minimized. Whereas when the coolant is injected at an angle to the mainstream flow, the coolant is more likely to remain attached to the platform.

With this vertical injection, there is a strong interaction of the coolant flow with the mainstream flow (including the passage-induced secondary flow). The formation and migration of the passage vortex across the passage is clearly seen by the measured film-cooling effectiveness. Because of this strong interaction of the coolant with the mainstream, the film-cooling-effectiveness distribution through the passage is very nonuniform from the leading edge to the trailing edge of the passage.

B. Redirected Injection

The film-cooling effectiveness measured on the platform with the upstream seal redirecting the coolant is shown in Fig. 6. As with the previous geometry, the film effectiveness is measured on the platform with four different coolant flow rates. The general behavior of the coolant being carried by the passage vortex from the pressure side to the suction side of the passage is still apparent. However, with the present configuration, the coolant exits the seal more uniformly than with the previous case. At the lowest flow rate of 0.5%, the protection offered by this seal redirecting the coolant is equitable to the seal that injects the coolant vertically onto the platform.

At the increased coolant flow rates, the effectiveness trends vary significantly from those of the vertical injection. The film-cooling effectiveness is more uniform across the passage, but the effectiveness decays rapidly through the passage. Almost immediately downstream of the slot, the effectiveness drops from 1.0 to approximately 0.6. The coolant exits the slot more uniformly, at the expense of the effectiveness rapidly decaying. With this more advanced flow configuration, the severe effects of vertical injection are reduced, and so the coolant more readily remains attached to the platform.

C. Labyrinth Injection

Figure 7 shows the film-effectiveness distributions measured with the most advanced stator–rotor seal: a labyrinthlike seal. The effectiveness distributions for this most complex seal configuration are very similar to those with the coolant redirection (Fig. 6). This might be anticipated, because the two configurations are identical near the exit of the seal. The effect of the passage-induced secondary flow remains very obvious, most notably at the lower flow rates. However, with the more complex labyrinthlike seal, the film-cooling effectiveness is reduced through the passage.

As it is likely anticipated, increasing the complexity of the seal configuration reduces the film-cooling effectiveness on the blade platform (Figs. 5–7). The point is reiterated by comparing the present configurations to the more idealistic inclined slot [27]. With all three of the present configurations, the effectiveness immediately downstream of the slot quickly decays; this is due to the injection of the coolant nearly perpendicular to the mainstream flow.

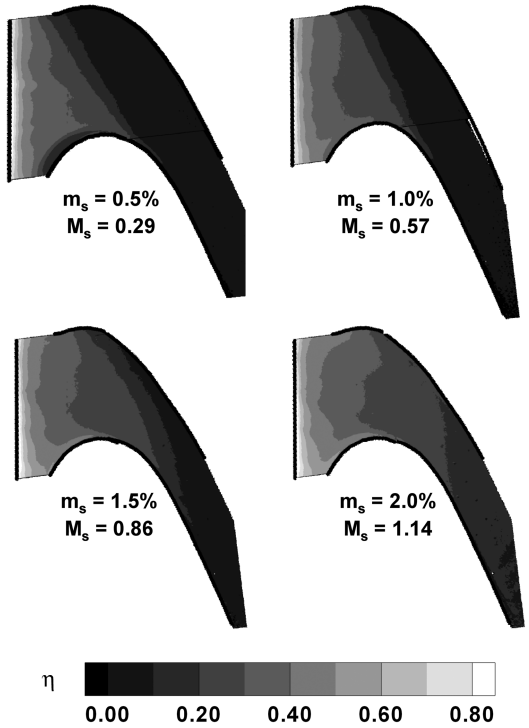

Fig. 7 Measured film-cooling effectiveness with labyrinth upstream injection.

Depending on the amount of coolant through the seal, the passage vortex strongly influences the behavior of the coolant remaining near the platform. With lower flow rates (less momentum flows), the coolant is carried by the passage vortex from the pressure side of the passage to the suction side. When the coolant flow rate is increased, the effect of the passage vortex is weakened, and the coolant covers a larger area of the passage, extending nearly to the trailing edge of the blades.

D. Laterally Averaged Effectiveness

For more direct comparisons of the different seal configurations, the laterally averaged film-cooling effectiveness is plotted in Figs. 8–11. The three configurations of the present investigation are considered, along with the fundamental inclined slot from Wright et al. [27] (in which the mainstream and coolant flows are identical to those of the current study). Figure 8 shows the effect of the coolant flow rate on the film-cooling effectiveness for each seal configuration. The leading edge of the blades is located at $x = 0$. As shown in Fig. 3, the seals of the present study are located upstream of the leading edge, and thus the effectiveness is plotted upstream of $x = 0$. As shown in Fig. 8, increasing the coolant flow rate increases the effectiveness through the passage for all seal configurations. The film-cooling effectiveness for the three current geometries decays rapidly from the initial injection, and this was clearly shown with the previously discussed contour plots.

Figure 9 shows the effect of the seal configuration at each of the given flow rates. These plots clearly indicate how the effectiveness on the platform decreases with the more advanced geometries. At the lowest coolant flow rate of 0.5%, the three current configurations produce the same level of cooling protection. The film effectiveness quickly diminishes as the coolant is whisked away by the passage vortex. Increasing the coolant flow rates produces marginal variations between the present seal configurations. However, for all four coolant flow rates, the film effectiveness for these advanced configurations is significantly lower than for the incline slot. This plot also clearly shows why the incline slot is advantageous: as the film effectiveness decreases through the passage, the decline is not as severe as with the advanced seals. Although the effectiveness decreases quickly from the seal, it should be noted that with the seals located upstream of the blades, more area is covered by the coolant.

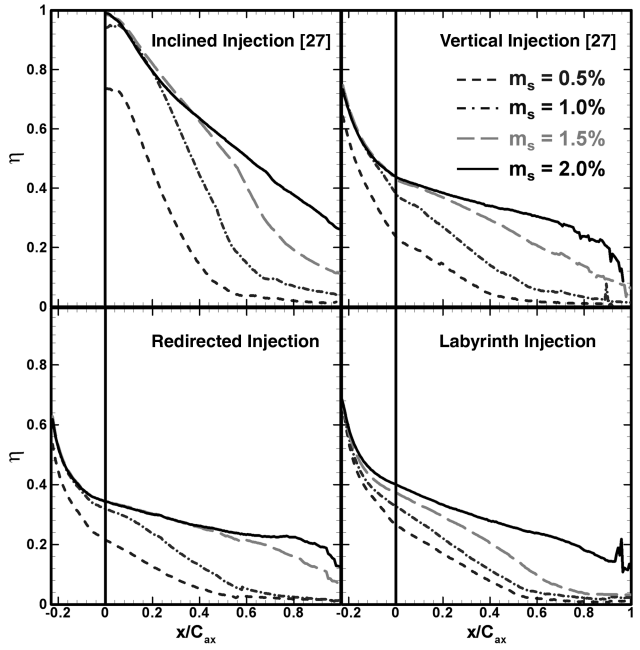

Fig. 8 Laterally averaged film-cooling effectiveness on the passage endwall for different seal configurations (coolant flow rate effect).

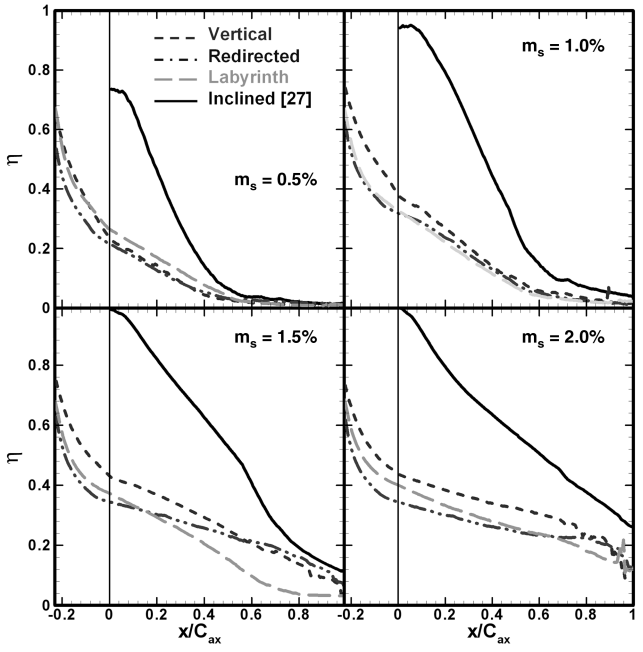

Fig. 9 Laterally averaged film-cooling effectiveness on the passage endwall for different coolant flow rates (seal configuration effect).

At the highest flow rates, the purge gas covers the entire passage from upstream to the trailing edge of the blades.

Figures 10 and 11 show the laterally averaged film-cooling effectiveness plotted versus $x/M_s s$. It must be noted that coordinates for the current configurations were adjusted, and so the exit of the seal is considered the starting point ($x = 0$). This was for a more direct comparison with other slot configurations. As Fig. 10 shows, the flow rate (blowing ratio) effect is eliminated from the laterally averaged effectiveness. In addition to the three present configurations and the previous inclined slot [27], the measured effectiveness is also compared with the most ideal case of tangential slot injection over a flat plate [36]. As explained by Wright et al. [27], the averaged effectiveness near the slot collapses with the established correlation near the slot (Fig. 10a). However, downstream of the slot, the effectiveness on the platform drops quickly, due to the

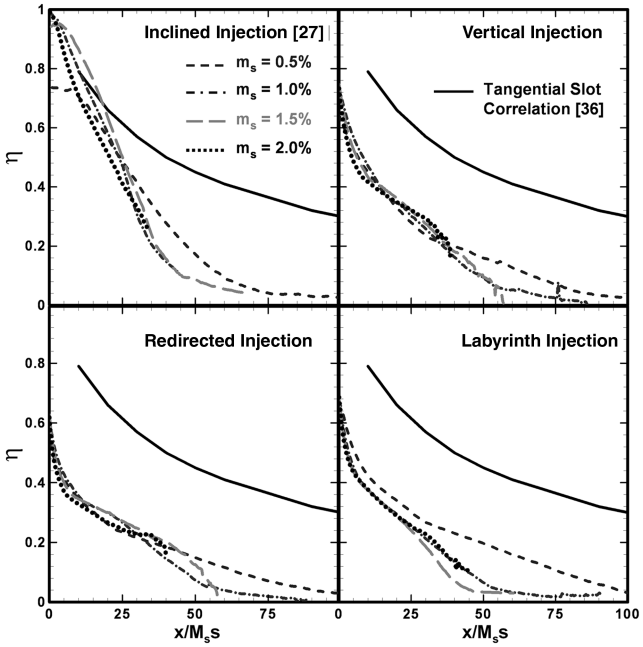

Fig. 10 Laterally averaged film-cooling effectiveness on the passage endwall for different seal configurations (coolant flow rate effect).

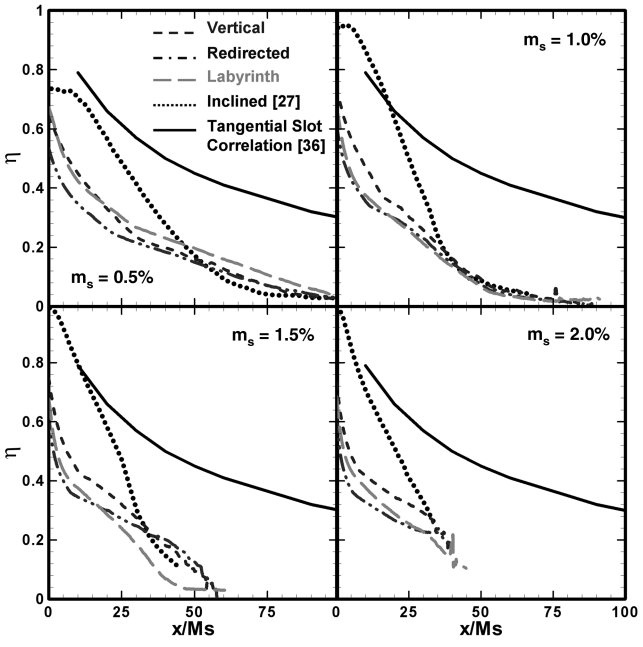

Fig. 11 Laterally averaged film-cooling effectiveness on the passage endwall for different coolant flow rates (seal configuration effect).

passage-induced secondary flow. Comparing the three current seals, even near the seal, the effectiveness is significantly lower than with the tangential injection. This is understood to be due to the nearly vertical injection of the coolant into the mainstream. Finally, the effect of each seal configuration can be seen in Fig. 11. As the figure clearly shows, the vertical, redirected, and labyrinth seals yield the same level of protection, and the film effectiveness from these seals is much lower than the inclined slot and the tangential slot.

V. Conclusions

Pressure-sensitive paint has again proven to be a valuable tool to obtain detailed film-cooling-effectiveness distributions. The PSP technique was used to measure the film-cooling effectiveness on a turbine-blade platform (within a five-blade linear cascade) for three different stator–rotor seals. The seals were chosen as a move away from idealistic configurations to more enginelike configurations. The effectiveness was measured for vertical coolant injection, coolant redirection, and injection from a labyrinthlike seal. In addition to changing the seal configuration, the coolant flow rate was also varied.

The more advanced configurations of the current study yield reduced film-cooling effectiveness compared with more idealistic configurations (i.e., inclined and tangential slot configurations). Increasing the coolant flow gives more uniform film-effectiveness distributions for the most advanced redirection and labyrinth configurations. However, increasing the flow rates leads to increased nonuniformity of the film-cooling effectiveness on the platform with vertical injection upstream of the blades.

Although the effectiveness is reduced through the passage with these more realistic designs, the flow of the coolant from the seal is more uniform across the length of the seal. In other words, the coolant exits over the entire length of the slot, which was not observed with the previous inclined slot (most notably at low flow rates); this contrasting exit behavior is the combined impact of both the seal geometry and the location of the seal relative to the leading edge of the blades. This offers positive information for designers, because the likelihood of ingestion is reduced with the seal located further upstream of the blades. To make a more fair comparison, the effectiveness distributions should be obtained with an inclined slot located further upstream of the blades.

This experimental study has attempted to close the gap between idealistic laboratory investigations and actual engine designs. However, more work is needed to further close the gap. The current study focused only on the protection offered by upstream injection, whereas most platform-cooling schemes consist of upstream injection combined with downstream discrete film-cooling holes. Future studies will include the combined effect of purge flow from advanced seal configurations and downstream discrete film cooling. In addition, the effect of increased freestream turbulence will be considered to more closely replicate actual platform-cooling conditions.

Acknowledgments

This publication was prepared with the support of the U.S. Department of Energy (DOE), Office of Fossil Energy, National Energy Technology Laboratory. However, any opinions, findings, conclusions, or recommendations expressed herein are those of the authors and do not necessarily reflect the views of the DOE.

References

[1] Han, J. C., Dutta, S., and Ekkad, S. V., *Gas Turbine Heat Transfer and Cooling Technology*, Taylor and Francis, New York, 2000, p. 646.

[2] Chyu, M. K., "Heat Transfer Near Turbine Nozzle Endwall," *Annals of the New York Academy of Sciences*, Vol. 934, No. 1, 2001, pp. 27–36.

[3] Langston, L. S., Nice, L. M., and Hooper, R. M., "Three-Dimensional Flow Within a Turbine Cascade Passage," American Society of Mechanical Engineers, Paper 76-GT-50, 1976.

[4] Langston, L. S., "Crossflows in a Turbine Cascade Passage," *Journal of Engineering for Power*, Vol. 102, Oct. 1980, pp. 866–874.

[5] Goldstein, R. J., and Spores, R. A., "Turbulent Transport on the Endwall in the Region Between Adjacent Turbine Blades," *Journal of Heat Transfer*, Vol. 110, No. 4A, Nov. 1988, pp. 862–869.

[6] Blair, M. F., "An Experimental Study of Heat Transfer and Film Cooling on Large-Scale Turbine Endwall," *Journal of Heat Transfer*, Vol. 96, Nov. 1974, pp. 524–529.

[7] Graziani, R. A., Blair, M. F., Taylor, J. R., and Mayle, R. E., "An Experimental Study of Endwall and Airfoil Surface Heat Transfer in a Large Scale Turbine Blade Cascade," *Journal of Engineering for Power*, Vol. 102, Apr. 1980, pp. 257–267.

[8] York, R. E., Hylton, L. D., and Mihelc, M. S., "An Experimental Investigation of Endwall Heat Transfer and Aerodynamics in a Linear Vane Cascade," *Journal of Engineering for Gas Turbines and Power*," Vol. 106, Jan. 1984, pp. 159–167.

[9] Thole, K. A., Radomsky, R. W., Kang, M. B., and Kohli, A., "Elevated Freestream Turbulence Effects on Heat Transfer for a Gas Turbine Vane," *International Journal of Heat and Fluid Flow*, Vol. 23, No. 2, 2002, pp. 137–147.

[10] Kwak, J. S., Lee, J. H., and Han, J. C., "Heat Transfer and Pressure Distributions on a Gas Turbine Vane End-Wall," *Proceedings of the Twelfth International Heat Transfer Conference*, International Centre for Heat and Mass Transfer, Ankara, Turkey, 2002, pp. 693–698.

[11] Takeishi, K., Matsuura, M., Aoki, S., and Sato, T., "An Experimental Study of Heat Transfer and Film Cooling on Low Aspect Ratio Turbine Nozzles," *Journal of Turbomachinery*, Vol. 112, July 1990, pp. 488–496.

[12] Harasgama, S. P., and Burton, C. S., "Film Cooling Research on the Endwall of a Turbine Nozzle Guide Vane in a Short Duration Annular Cascade, Part 1: Experimental Technique and Results," *Journal of Turbomachinery*, Vol. 114, Oct. 1992, pp. 734–740.

[13] Jabbari, M. Y., Marston, K. C., Eckert, E. R. G., and Goldstein, R. J., "Film Cooling of the Gas Turbine Endwall by Discrete-Hole Injection," *Journal of Turbomachinery*, Vol. 118, Apr. 1996, pp. 278–284.

[14] Friedrichs, S., Hodson, H. P., and Dawes, W. N., "Distribution of Film Cooling Effectiveness on a Turbine Endwall Measured Using the Ammonia and Diazo Technique," *Journal of Turbomachinery*, Vol. 118, Oct. 1996, pp. 613–621.

[15] Friedrichs, S., Hodson, H. P., and Dawes, W. N., "Aerodynamic Aspects of Endwall Film Cooling," *Journal of Turbomachinery*, Vol. 119, Oct. 1997, pp. 786–793.

[16] Friedrichs, S., Hodson, H. P., and Dawes, W. N., "The Design of an Improved Endwall Film Cooling Configuration," American Society of Mechanical Engineers, Paper 98-GT-483, 1998.

[17] Barigozzi, G., Benzoni, G., Franchini, G., and Derdichizzi, A., "Fan-Shaped Hole Effects on the Aero-Thermal Performance of a Film Cooled Endwall," American Society of Mechanical Engineers, Paper GT2005-68544, 2005.

[18] Roy, R. P., Squires, K. D., Gerendas, M., Song, S., Howe, W. J., and Ansari, A., "Flow and Heat Transfer at the Hub Endwall of Inlet Vane Passages—Experiments and Simulations," American Society of Mechanical Engineers, Paper 2000-GT-198, 2000.

[19] Burd, S. W., Satterness, C. J., and Simon, T. J., "Effects of Slot Bleed Injection over a Contoured Endwall on Nozzle Guide Vane Cooling Performance, Part 2: Thermal Measurements," American Society of Mechanical Engineers, Paper 2000-GT-200, 2000.

[20] Oke, R., Simon, T., Shih, T., Zhu, B., Lin, Y. L., and Chyu, M., "Measurements over a Film-Cooled Contoured Endwall with Various Coolant Injection Rates," American Society of Mechanical Engineers, Paper 2001-GT-0140, 2001.

[21] Oke, R. A., and Simon, T. W., "Film Cooling Experiments with Flow Introduced Upstream of a First Stage Nozzle Guide Vane through Slots of Various Geometries," American Society of Mechanical Engineers, Paper GT-2002-30169, 2002.

[22] Nicklas, M., "Film-Cooled Turbine Endwall in a Transonic Flow Filed, Part 2: Heat Transfer and Film Cooling Effectiveness," *Journal of Turbomachinery*, Vol. 123, Oct. 2001, pp. 720–729.

[23] Liu, G., Liu, S., Zhu, H., Lapworth, B. C., and Forest, A. E., "Endwall Heat Transfer and Film Cooling Measurements in a Turbine Cascade with Injection Upstream of Leading Edge," *Heat Transfer, Asian Research*, Vol. 33, May 2004, pp. 141–152.

[24] Zhang, L. J., and Jaiswal, R. S., "Turbine Nozzle Endwall Film Cooling Study Using Pressure-Sensitive Paint," *Journal of Turbomachinery*, Vol. 123, Oct. 2001, pp. 730–738.

[25] Zhang, L. J., and Moon, H. K., "Turbine Nozzle Endwall Inlet Film Cooling—The Effect of a Backward Facing Step," American Society of Mechanical Engineers, Paper GT2003-38319, 2003.

[26] Knost, D. G., and Thole, K. A., "Adiabatic Effectiveness Measurements of Endwall Film Cooling for a First Stage Vane," American Society of Mechanical Engineers, Paper GT2004-53326, 2004.

[27] Wright, L. M., Gao, Z., Yang, H., and Han, J. C., "Film Cooling Effectiveness Distribution on a Gas Turbine Blade Platform with Inclined Slot Leakage and Discrete Film Hole Flows," American Society of Mechanical Engineers, Paper GT2006-90375, 2006.

[28] Zhang, L., and Han, J. C., "Influence of Mainstream Turbulence on Heat Transfer Coefficients from a Gas Turbine Blade," *Journal of Heat Transfer*, Vol. 116, Nov. 1994, pp. 896–903.

[29] Wright, L. M., Gao, Z., Varvel, T. A., and Han, J. C., "Assessment of Steady State PSP, TSP, and IR Measurement Techniques for Flat Plate Film Cooling," American Society of Mechanical Engineers, Paper HT2005-72363, 2005.

[30] Gao, Z., Wright, L. M., and Han, J. C., "Assessment of Steady State PSP and Transient IR Measurement Techniques for Leading Edge Film Cooling," American Society of Mechanical Engineers, Paper IMECE2005-80146, 2005.

[31] Ahn, J., Schobeiri, M. T., Han, J. C., and Moon, H. K., "Film Cooling Effectiveness on the Leading Edge of a Rotating Turbine Blade," American Society of Mechanical Engineers, Paper IMECE2004-59852, 2004.

[32] Ahn, J., Schobeiri, M. T., Han, J. C., and Moon, H. K., "Film Cooling Effectiveness on the Leading Edge of a Rotating Film-Cooled Blade Using Pressure-Sensitive Paint," American Society of Mechanical Engineers, Paper GT2005-68344, 2005.

[33] Ahn, J., Mhetras, S., and Han, J. C., "Film-Cooling Effectiveness on a Gas Turbine Blade Tip Using Pressure-Sensitive Paint," American Society of Mechanical Engineers, Paper GT2004-53249, 2004.

[34] Mhetras, S., Yang, H., Gao, Z., and Han, J. C., "Film-Cooling Effectiveness on Squealer Rim Walls and Squealer Cavity Floor of a Gas Turbine Blade Tip Using Pressure-Sensitive Paint," American Society of Mechanical Engineers, Paper GT2005-68387, 2005.

[35] Coleman, H. W., and Steele, W. G., *Experimentation and Uncertainty Analysis for Engineers*, Wiley, New York, 1989.

[36] Goldstein, R. G., "Film Cooling," *Advances in Heat Transfer*, Vol. 7, 1971, pp. 321–379.